Open Journal of Mathematical Sciences

PSR Press

Article

An analytical method for finding exact solutions of a nonlinear partial differential equation arising in electrical engineering

Md. Nur Alam

Department of Mathematics, Pabna University of Science & Technology, Pabna-6600, Bangladesh;
nuralam.pstu23@gmail.com; nuralam23@pust.ac.bd

Academic Editor: Haitao Qi
Received: 12 September 2022; Accepted: 15 February 2023; Published: 31 March 2023.

Abstract: In this investigation, we aim to investigate the novel exact solutions of nonlinear partial differential equations (NLPDEs) arising in electrical engineering via the -expansion method. New acquired solutions are kink, particular kink, bright, dark, periodic combined-dark bright and combined-dark singular solitons, and hyperbolic functions solutions. The achieved distinct types of solitons solutions contain critical applications in engineering and physics. Numerous novel structures (3D, contour, and density plots) are also designed by taking the appropriate values of involved parameters. These solutions express the wave show of the governing models, actually.

Keywords: Analytical method; MZK equation; Electrical engineering; Exact solution.

MSC: 35E05; 35C08; 35Q51; 37L50; 37J25; 33F05.

1. Introduction

Current nonlinear science, mathematical physics, and engineering phenomena are associated with NLPDEs. These are much meaningful in describing everyday difficulties arising in nonlinear science and nature, such as computer science, waves, biology, geology, birefringent fibers, population ecology, fluid dynamics, solid-state physics, wave propagation, and many more. Numerous mathematical procedures have been efficiently implemented to investigate the important results of NLPDEs [1–23]. Utilizing these procedures, numerous new features of wave performance of these NLPDEs have been found. The results have much influence on diverse experimental phenomena such as long-distance high-speed transmission lines, optics, and optics as temporal or spatial optical solitons and optical fibers.

The purpose of this paper is to give the $(\Psi - \Phi)$-expansion method [24] and the Hamiltonian system [25,26] to determine ESs for a discrete non-linear transmission line model [27–29]. The proposed equation is also known via the MZK model that assistances in defining the device of various characteristics [30–33] and describes the evolution of weakly non-linear ion-acoustic waves in a plasma involving hot iso-thermal electrons and cold-ions in the existence of a uniform-magnetic field in the x-direction. NLPDEs have been deliberate as essential in numerous applications. The proposed equation has been implemented to define natural, mechanical, multiple physical phenomena, and engineering. That performs because it contains beforehand unknown multi-variable tasks and their derivatives, such as the electrical transmission lines, which are proposed as a good standard of systems for examining non-linear excitations, behave inside non-linear media, as nominated in Figure 1.

The nonlinear electrical transmission line is proposed based on periodically loading with var-actors or organizing inductors and var-actors in a 1D lattice. The nonlinear network with some couple nonlinear LC with a dispersive transmission line has consisted of this equation. Numerous identical dispersive lines are coupled with capacitance C_s at each node, as denoted in Figure 1, where a conductor L and a nonlinear capacitor of capacitance $C\left(v_{p,q}\right)$ are in each line in the shunt branch. The scientific equation which denotes the discrete

nonlinear transmission is given via the MZK equation that is defined through Duan when he applied the Kirchhoff law on the equation, which as

$$\frac{\partial^2 R_{p,q}}{\partial S^2} = \frac{1}{L}\left(V_{p+1,q} - 2V_{p,q} + V_{p-1,q}\right) + C_s \frac{\partial^2}{\partial S^2}\left(V_{p,q+1} - 2V_{p,q} + V_{p,q-1}\right), \tag{1}$$

where $V_{p,q} = V_{p,q}(S)$ is the voltage so that the non-linear charge is find as

$$R_{p,q} = C_0\left(V_{p,q} + \frac{\alpha_1}{2}V^2{}_{p,q} + \frac{\alpha_2}{3}V^3{}_{p,q}\right), \tag{2}$$

where α_1,α_2 are arbitrary constants. Substituting Eq. (2) into Eq. (1), we have

$$C_0\frac{\partial^2}{\partial S^2}\left(V_{p,q} + \frac{\alpha_1}{2}V^2{}_{p,q} + \frac{\alpha_2}{3}V^3{}_{p,q}\right) = \frac{1}{L}\left(V_{p+1,q} - 2V_{p,q} + V_{p+1,q}\right) + C_s\frac{\partial^2}{\partial S^2}\left(V_{p,q+1} - 2V_{p,q} + V_{p,q-1}\right). \tag{3}$$

Replacing $V_{p,q}(S) = V(p,q,S)$, leads to

$$C_0\frac{\partial^2}{\partial S^2}\left(V + \frac{\alpha_1}{2}V^2 + \frac{\alpha_2}{3}V^3\right) = \frac{1}{L}\frac{\partial^2}{\partial p^2}\left(V + \frac{1}{12}\frac{\partial^2}{\partial p^2}\right) + C_s\frac{\partial^4}{\partial S^2\partial q^2}\left(V + \frac{1}{12}\frac{\partial^2 V}{\partial q^2}\right). \tag{4}$$

Based on the reductive perturbation technique, Eq. (4) is reduced to the following model:

$$\varphi_t + f_1\varphi\varphi_x + q\varphi^2\varphi_x + d\varphi_{xxx} + g\varphi_{xyy} = 0, \tag{5}$$

where $y = \sqrt{\gamma}q$, $x = \sqrt{\gamma}(p - \nu_s S)$, $t = \sqrt{\gamma}S$, $V(p,q,S) = \gamma\varphi(x,y,t)$, $\nu_s^2 = \frac{1}{LC_0}$, $f_1 = -\alpha_1\nu_s$, $q = -\alpha_2\nu_s$, $d = \frac{1}{24\alpha\alpha_1 L\nu_s}$, $g = \frac{\alpha_1}{288L^2\nu_s C_0^2}$.

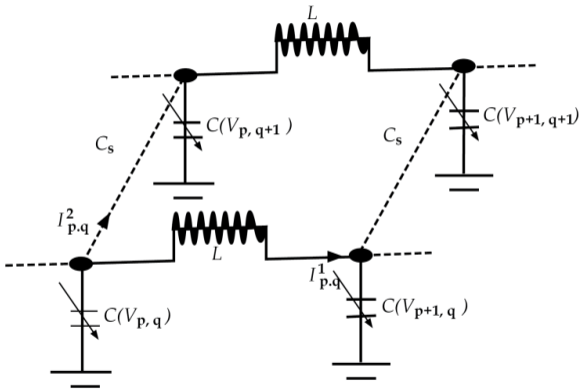

Figure 1. Linear representation of the nonlinear electrical transmission line.

2. Description of the $(\Psi - \Phi)$-expansion method

Consider

$$P(\hbar,\ \hbar_x, \hbar_{x\,x}, \hbar_t, \hbar_{t\,t}, \hbar_{\mathrm{xt}}., ...) = 0, \tag{6}$$

where is a polynomial in $\hbar$ as well as its derivatives.

Firstly, use the traveling variable:

$$\hbar = \hbar(x,\ t) = \hbar(\chi),\ \chi = p_3(x - \mathrm{Vt}), \tag{7}$$

wherep_3 and V are a constant to be determine later. Using (7) into (6), we get

$$R(\hbar,\ p_3\hbar^{'}, p_3^2\hbar^{''}, -p_3V\hbar^{'}, p_3^2V^2\hbar^{''}, -p_3^2V^2\hbar^{''}, ...) = 0. \tag{8}$$

Secondly, consider

$$\hbar(\chi) = \sum_{i=0}^{M} S_i\Psi^i + \sum_{i=1}^{M} T_i\Psi^{i-1}\Phi, \tag{9}$$

where $\Psi = (\Theta^{'}/\Theta)$ and $\Phi = (\Omega^{'}/\Omega)$. Now $\Theta = \Theta(\chi)$ and $\Omega = \Omega(\chi)$ are represent as

$$\Theta^{'}(\chi) = -\Theta(\chi)\,\Omega(\chi),$$
$$\Omega^{'}(\chi) = 1 - \,\Omega(\chi)^2,$$

where $\Theta(\chi) = \pm sech(\chi)$, $\Omega(\chi) = \tanh(\chi)$, $\Theta(\chi) = \pm csch(\chi)$, $\Omega(\chi) = \coth(\chi)$.

Thirdly, a polynomial in Ψor Φ accomplised plugging Eq. (9) into Eq. (8). Defining the constant values of the corresponding power of Ψor Φ yields a system of equations, which might be defined to make S_i and T_i. After getting S_i and T_i in (9), the answers of the studied model complete the intention of the answers of the proposed model.

3. Mathematical analysis

Since x, y, t are independent transformation variables. Employing $\varphi = \varphi(x,y,t) = \varphi(\eta)$, where $\eta = k_1x + k_2y + k_3t$ into equation (5), we have

$$6k_3\varphi + 3f_1k_1\varphi^2 + 2\mathrm{qk}_1\varphi^3 + 6k_1\left(\mathrm{dk}_1^2 + \mathrm{gk}_2^2\right)\varphi^{''} = 0. \tag{10}$$

According the studied technique which we discuss in §2, we find

$$\hbar(\chi) = S_0\Psi^0 + S_1\Psi^1 + T_1\Psi^0\Phi = S_0 + \frac{T_1}{\Omega} - (S_1 + T_1)\,\Omega\,. \tag{11}$$

Collecting the coefficient of Ψ and Φ and solving the resulting system, we get

Cluster I: Substituting $k_2 = \pm\sqrt{\frac{-24dqk_1^2+f_1^2}{24gq}}$, $k_3 = \frac{1}{6}\frac{f_1^2k_1}{q}$, $S_0 = -\frac{f_1}{2q}$,$S_1 = -\frac{f_1}{2q}$,$T_1 = 0$ in Eq. (11), we get

$$\hbar_1(x,y,t) = -\frac{f_1}{2q} + \frac{f_1}{2q} \times \tanh(k_1x + k_2y + k_3t),$$

and

$$\hbar_2(x,y,t) = -\frac{f_1}{2q} + \frac{f_1}{2q} \times \coth(k_1x + k_2y + k_3t).$$

Cluster II: Substituting $k_2 = \pm\sqrt{\frac{-24dqk_1^2+f_1^2}{24gq}}$, $k_3 = \frac{1}{6}\frac{f_1^2k_1}{q}$, $S_0 = -\frac{f_1}{2q}$ and $S_1 = \frac{f_1}{2q}$,$T_1 = 0$ in Eq. (11), we get

$$\hbar_3(x,y,t) = -\frac{f_1}{2q} - \frac{f_1}{2q} \times \tanh(k_1x + k_2y + k_3t),$$

and

$$\hbar_4(x,y,t) = -\frac{f_1}{2q} - \frac{f_1}{2q} \times \coth(k_1x + k_2y + k_3t).$$

Cluster III: Substituting $k_2 = \pm\sqrt{\frac{-96dqk_1^2-f_1^2}{96gq}}$, $k_3 = \frac{1}{6}\frac{f_1^2k_1}{q}$, $S_0 = -\frac{f_1}{2q}$ and $S_1 = -\frac{f_1}{2q}$,$T_1 = \frac{f_1}{4q}$ in Eq. (11), we get

$$\hbar_5(x,y,t) = -\frac{f_1}{2q} + \frac{f_1}{2q} \times \tanh(k_1x + k_2y + k_3t) + \frac{f_1}{4q}\left(\frac{1}{\tanh(k_1x + k_2y + k_3t)} - \tanh(k_1x + k_2y + k_3t)\right),$$

and

$$\hbar_6(x,y,t) = -\frac{f_1}{2q} + \frac{f_1}{2q} \times \coth(k_1x + k_2y + k_3t) + \frac{f_1}{4q}\left(\frac{1}{\tanh(k_1x + k_2y + k_3t)} - \tanh(k_1x + k_2y + k_3t)\right).$$

Cluster IV: Substituting $k_2 = \pm\sqrt{\frac{-24dqk_1^2 - f_1^2}{24gq}}$, $k_3 = \frac{1}{6}\frac{f_1^2 k_1}{q}$, $S_0 = -\frac{f_1}{2q}$ and $S_1 = -\frac{f_1}{2q}$,$T_1 = \frac{f_1}{2q}$ in Eq. (11), we get

$$\hbar_7(x,y,t) = -\frac{f_1}{2q} + \frac{f_1}{2q} \times \tanh(k_1x + k_2y + k_3t) + \frac{f_1}{4q}\left(\frac{1}{\tanh(k_1x + k_2y + k_3t)} - \tanh(k_1x + k_2y + k_3t)\right),$$

and

$$\hbar_8(x,y,t) = -\frac{f_1}{2q} + \frac{f_1}{2q} \times \coth(k_1x + k_2y + k_3t) + \frac{f_1}{4q}\left(\frac{1}{\tanh(k_1x + k_2y + k_3t)} - \tanh(k_1x + k_2y + k_3t)\right).$$

4. Numerical simulations

In this study, we effectively construct novel solitons and hyperbolic and trigonometric function solutions for the proposed model using the $(\Psi - \Phi)$-expansion method. This technique is measured as the most recent scheme in this field, which has not been utilized in these equations earlier. For physical analysis, 3-D, 2-D, and contour plots of some of these solutions are comprised of suitable parameters. The obtained solutions discover their application in communication to convey information because solitons can spread over long distances without reduction and without changing their forms. We only included specific figures in this paper to avoid overloading the document. All the developed results are novel and distinct from the reported results. For graphical representation for the studied model, the physical behavior of $\hbar_1(x,y,t)$ using the proper values of parameters $k_1 = 2$, $f_1 = -1$, $f_2 = 1$, $y = 1$, $q = 2$, $d = 5$, and $g = 2$ are shown in Figures 2, 3 and 4. The physical behavior of $\hbar_2(x,y,t)$ using the appropriate values of parameters $k_1 = 2$, $f_1 = -1$, $f_2 = 1$, $y = 1$, $q = 2$, $d = 0.5$ and $g = 0.2$ are shown in Figures 5, 6 and 7.

The physical behavior of $\hbar_3(x,y,t)$ using the appropriate values of parameters $k_1 = 2$, $f_1 = 20$, $f_2 = 1$, $y = 1$, $q = 2$, $d = 1$ and $g = 2$ are shown in Figures 8, 9 and 10. The physical behavior of $\hbar_6(x,y,t)$ using the appropriate values of parameters $k_1 = 2$, $f_1 = -0.5$, $f_2 = 1$, $y = 1$, $q = 2$, $d = 1$ and $g = 2$ are shown in Figures 11, 12 and 13. The physical behavior of $\hbar_7(x,y,t)$ using the appropriate values of parameters $k_1 = 2$, $f_1 = -0.5$, $f_2 = 1$, $y = 1$, $q = 2$, $d = 5$ and $g = 2$ are shown in Figures 14, 15 and 16.

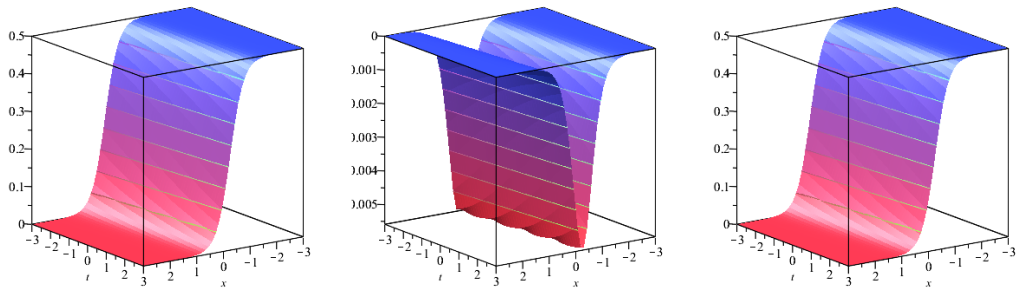

Figure 2. 3D graph (Real, Imaginary and absolute value plot) of the solution $\hbar_1\,(x, y,\ t)$ with $k_1 = 2$, $f_1 = -1$, $f_2 = 1, y = 1, q = 2, d = 5$ **and** $g = 2$.

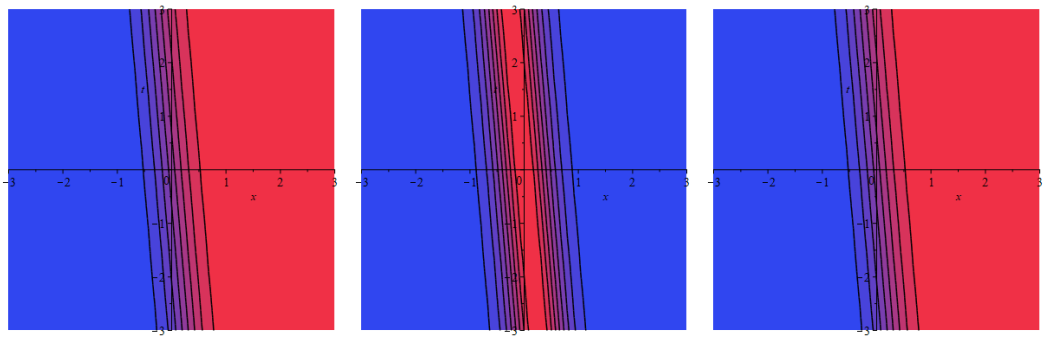

Figure 3. Contour graph (Real, Imaginary and absolute value plot) of the solution $\hbar_1\,(x, y,\ t)$ with $k_1 = 2$, $f_1 = -1$, $f_2 = 1, y = 1, q = 2, d = 5$ and $g = 2$.

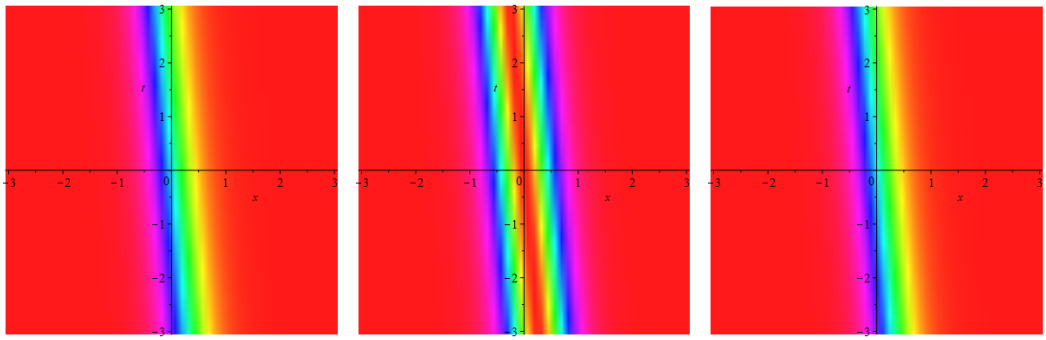

Figure 4. Density graph (Real, Imaginary and absolute value plot) of the solution $\hbar_1(x, y, t)$ with $k_1 = 2$, $f_1 = -1$, $f_2 = 1$, $y = 1$, $q = 2$, $d = 5$ and $g = 2$.

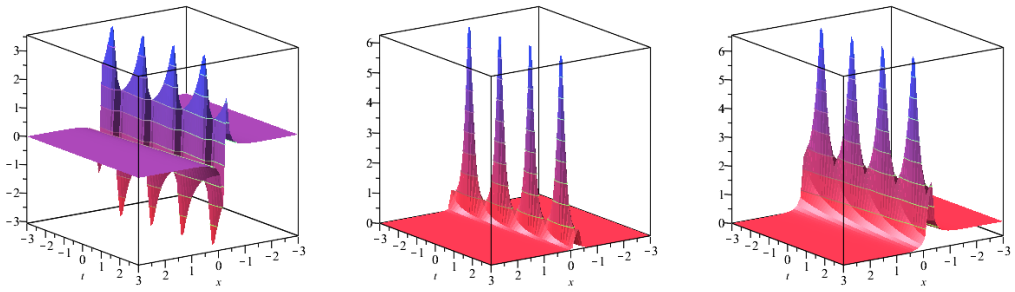

Figure 5. 3D graph (Real, Imaginary and absolute value plot) of the solution $\hbar_2(x, y, t)$ **with** $k_1 = 2$, $f_1 = -1$, $f_2 = 1$, $y = 1$, $q = 2$, $d = 0.5$ **and** $g = 0.2$.

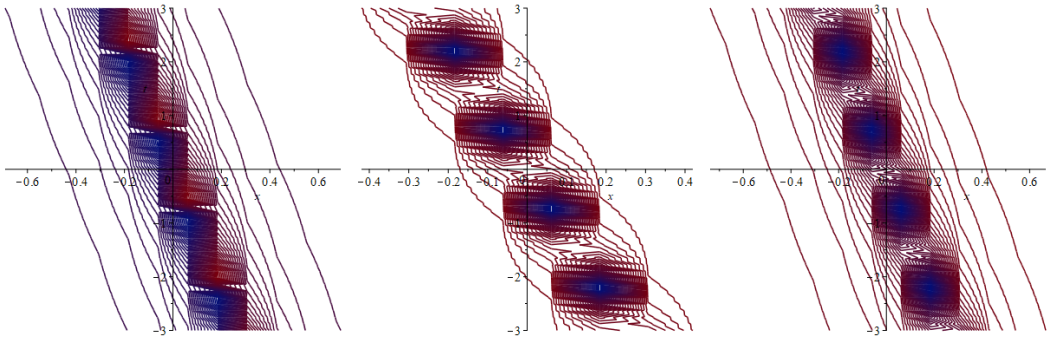

Figure 6. Contour graph (Real, Imaginary and absolute value plot) of the solution $\hbar_2(x, y, t)$ with $k_1 = 2$, $f_1 = -1$, $f_2 = 1$, $y = 1$, $q = 2$, $d = 0.5$ and $g = 0.2$.

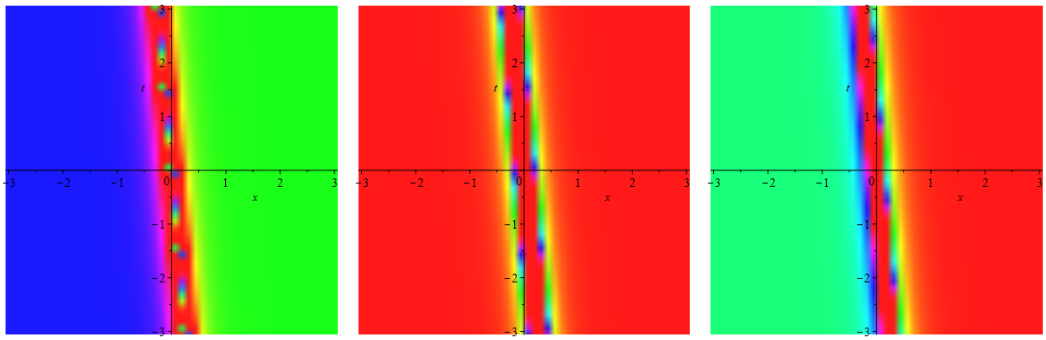

Figure 7. Density graph (Real, Imaginary and absolute value plot) of the solution $\hbar_2(x, y, t)$ with $k_1 = 2$, $f_1 = -1$, $f_2 = 1$, $y = 1$, $q = 2$, $d = 0.5$ and $g = 0.2$.

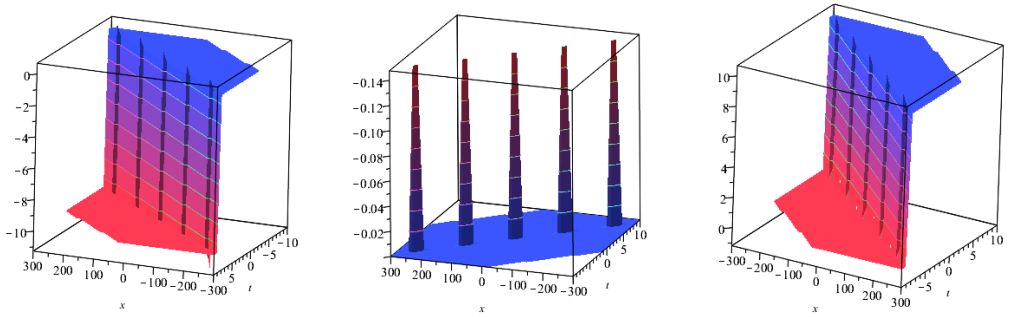

Figure 8. 3D graph (Real, Imaginary and absolute value plot) of the solution $\hbar_3(x, y, t)$ **with** $k_1 = 2$, $f_1 = 20$, $f_2 = 1, y = 1, q = 2, d = 1$ **and** $g = 2$.

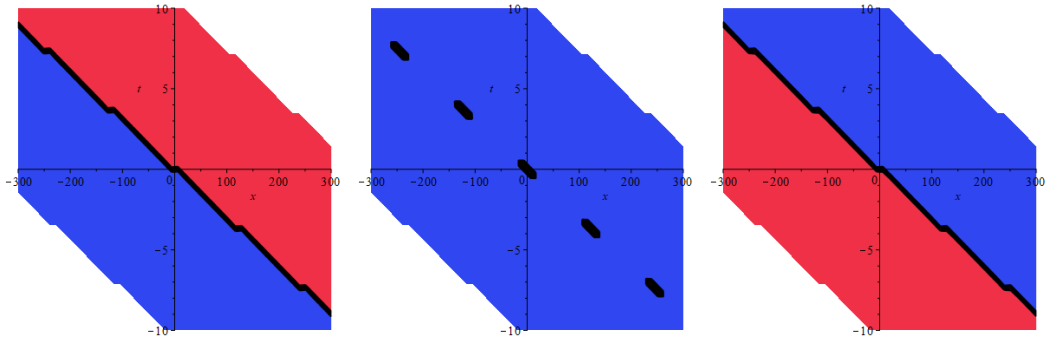

Figure 9. Contour graph (Real, Imaginary and absolute value plot) of the solution $\hbar_3(x, y, t)$ with $k_1 = 2$, $f_1 = 20$, $f_2 = 1, y = 1, q = 2, d = 1$ and $g = 2$.

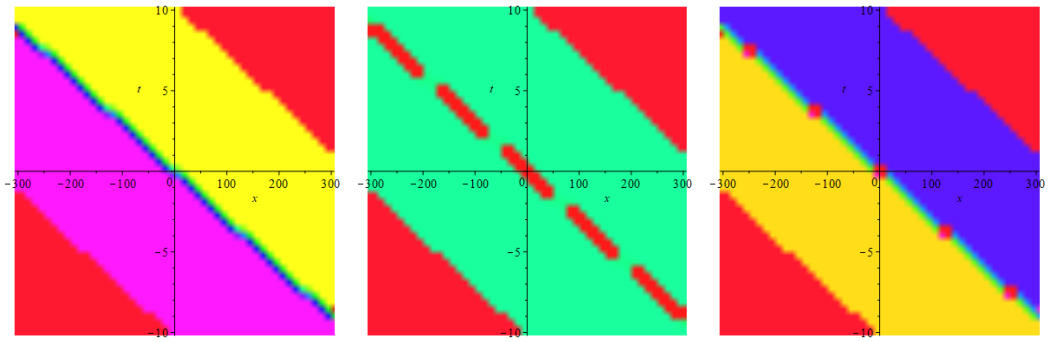

Figure 10. Density graph (Real, Imaginary and absolute value plot) of the solution $\hbar_3(x, y, t)$ with $k_1 = 2$, $f_1 = 20$, $f_2 = 1, y = 1, q = 2, d = 1$ and $g = 2$.

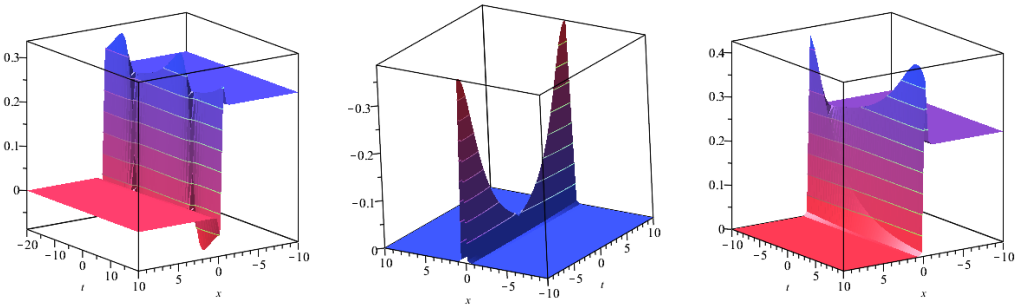

Figure 11. 3D graph (Real, Imaginary and absolute value plot) of the solution $\hbar_6(x, y, t)$ **with** $k_1 = 2$, $f_1 = -0.5$, $f_2 = 1, y = 1, q = 2, d = 1$ **and** $g = 2$

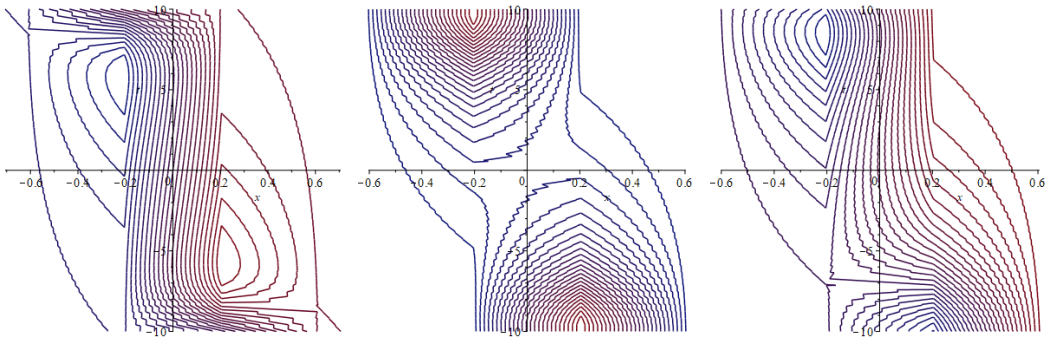

Figure 12. Contour graph (Real, Imaginary and absolute value plot) of the solution $\hbar_6(x, y, t)$ with $k_1 = 2$, $f_1 = -0.5$, $f_2 = 1$, $y = 1$, $q = 2$, $d = 1$ and $g = 2$.

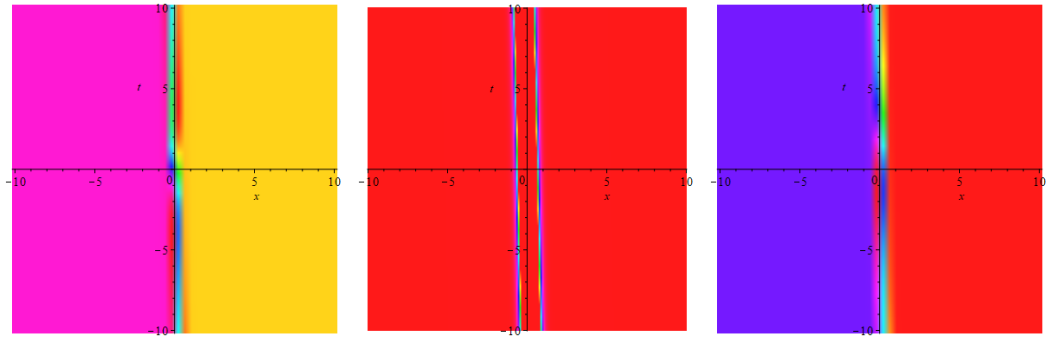

Figure 13. Density graph (Real, Imaginary and absolute value plot) of the solution $\hbar_6(x, y, t)$ with $k_1 = 2$, $f_1 = -0.5$, $f_2 = 1$, $y = 1$, $q = 2$, $d = 1$ and $g = 2$.

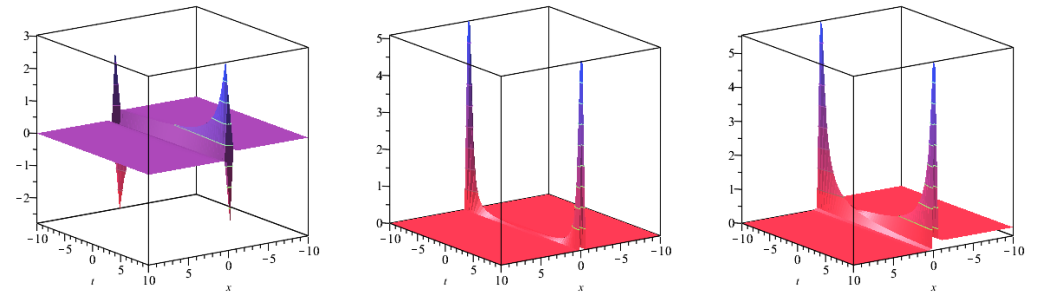

Figure 14. 3D graph (Real, Imaginary and absolute value plot) of the solution $\hbar_7(x, y, t)$ **with** $k_1 = 2$, $f_1 = -0.5$, $f_2 = 1$, $y = 1$, $q = 2$, $d = 5$ **and** $g = 2$.

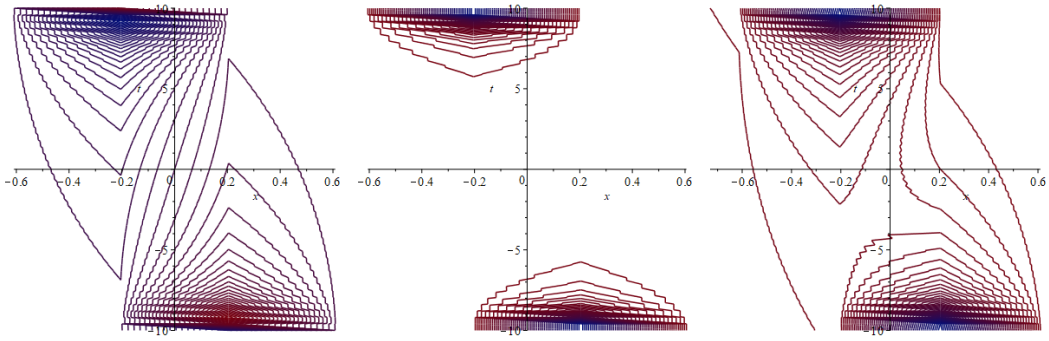

Figure 15. Contour graph (Real, Imaginary and absolute value plot) of the solution $\hbar_7(x, y, t)$ with $k_1 = 2$, $f_1 = -0.5$, $f_2 = 1$, $y = 1$, $q = 2$, $d = 5$ and $g = 2$.

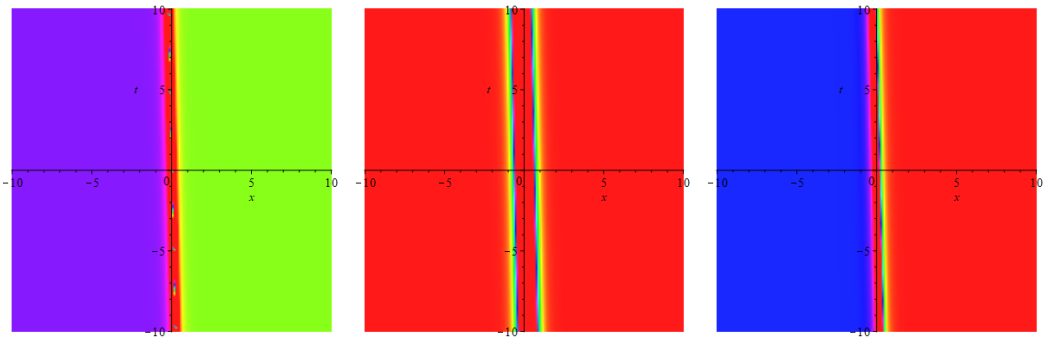

Figure 16. Density graph (Real, Imaginary and absolute value plot) of the solution $\hbar_7(x, y, t)$ with $k_1 = 2$, $f_1 = -0.5$, $f_2 = 1$, $y = 1$, $q = 2$, $d = 5$ and $g = 2$.

5. Conclusion

In this paper, we constructed new solitons solutions for the proposed model via the $(\Psi - \Phi)$-expansion method, in the form of kink, singular kink, bright, dark, mixed bright-dark solitons as well as hyperbolic, rational and trigonometric functions solutions. By choosing the suitable values of parameters and to better underst and the physical structures of the solutions, 3-d, contour and density graphs have been plotted. From the acquired results and figures, it is observed that all solutions demonstrated wave behavior. Also, these solutions yield traveling dark wave behaviors to the considered models, physically.

Acknowledgments: The author thanks to Faculty of Science, Pabna University of Science and Technology, Pabna-6600, Bangladesh for supporting project number (Project-2020/2021).

Conflicts of Interest: Declare conflicts of interest or state "The authors declare no conflict of interest."

References

[1] Jawad, A. J. A. M., Petkovic, M. D., & Biswas, A. (2010). Soliton solutions of a few nonlinear wave equations. *Applied Mathematics and Computation, 216*(9), 2649-2658.

[2] Deresse, A. T., Mussa, Y. O., & Gizaw, A.K. (2021). Analytical Solution of Two-Dimensional Sine-Gordon Equation. *Advances in Mathematical Physics*, 2021.

[3] Ahmad, H., Alam, M. N., & Omri, M. (2021). New computational results for a prototype of an excitable system. *Results in Physics, 28*, 104666.

[4] Wang, H., Alam, M. N., Ilhan, O. A., Singh, G., & Manafian, J. (2021). New complex wave structures to the complex Ginzburg-L andau model. *AIMS Mathematics, 6*(8), 8883-8894.

[5] Odabasi, M. Investigation of exact solutions of some nonlinear evolution equations via an analytical approach. *Mathematical Sciences and Applications E-Notes, 9*(2), 64-73.

[6] Lu, Q., Zhang, S., & Zheng, H. (2021). Exact solutions of a class of nonlinear dispersive long wave systems via Feng's first integral method. *AIMS Mathematics, 6*(8), 7984-8000.

[7] Rezazadeh, H., Vahidi, J., Zafar, A., & Bekir, A. (2020). The functional variable method to find new exact solutions of the nonlinear evolution equations with dual-power-law nonlinearity. *International Journal of Nonlinear Sciences and Numerical Simulation, 21*(3-4), 249-257.

[8] El-Shiekh, R. M. (2019). Classes of new exact solutions for nonlinear Schrödinger equations with variable coefficients arising in optical fiber. *Results in Physics, 13*, 102214.

[9] Alam, M. N., Akbar, M. A., & Mohyud-Din, S. T. (2013). A novel (G'/G)-expansion method and its application to the Boussinesq equation. *Chinese Physics B*, 23(2), 020203.

[10] Elsayed, M. Z., Yasser, A. A., & Reham, M. S. (2014). The improved generalized Riccati equation mapping method and its application for solving a nonlinear partial differential equation (PDE) describing the dynamics of ionic currents along microtubules. *Scientific Research and Essays, 9*(8), 238-248.

[11] Khater, M. M., Nofal, T. A., Abu-Zinadah, H., Lotayif, M. S., & Lu, D. (2021). Novel computational and accurate numerical solutions of the modified Benjamin–Bona–Mahony (BBM) equation arising in the optical illusions field. *Alex andria Engineering Journal, 60*(1), 1797-1806.

[12] Wazwaz, A. M. (2017). Exact soliton and kink solutions for new (3+1)-dimensional nonlinear modified equations of wave propagation. *Open Engineering, 7*(1), 169-174.

[13] Bekir, A., Zahran, E. H., & Shehata, M. S. (2020). The agreement between the new exact and numerical solutions of the 3D-fractional-Wazwaz-Benjamin-Bona-Mahony equation. *Journal of Science and Arts, 20*(2), 251-260.

[14] Kaabar, M. K., Kaplan, M., & Siri, Z. (2021). New exact soliton solutions of the $(3+1)$-dimensional conformable Wazwaz–Benjamin–Bona–Mahony equation via two novel techniques. *Journal of Function Spaces, 2021*, Article ID 4659905, 13 pages. https://doi.org/10.1155/2021/4659905.

[15] Liu, S. (2020). Multiple rogue wave solutions for the (3+ 1)-dimensional generalized Kadomtsev-Petviashvili Benjamin-Bona-Mahony equation. *Chinese Journal of Physics, 68*, 961-970.

[16] Zahran, E. H., Shehata, M. S., Mirhosseini-Alizamini, S. M., Alam, M. N., & Akinyemi, L. (2021). Exact propagation of the isolated waves model described by the three coupled nonlinear Maccari's system with complex structure. *International Journal of Modern Physics B, 35*(18), 2150193, https://doi.org/10.1142/S0217979221501939.

[17] Jhangeer, A., Faridi, W. A., Asjad, M. I., & Akgül, A. (2021). Analytical study of soliton solutions for an improved perturbed Schrödinger equation with Kerr law non-linearity in non-linear optics by an expansion algorithm. *Partial Differential Equations in Applied Mathematics, 4*, 100102, https://doi.org/10.1016/j.padiff.2021.100102.

[18] Faridi, W. A., Asjad, M. I., & Jhangeer, A. (2021). The fractional analysis of fusion and fission process in plasma physics. *Physica Scripta, 96*(10), 104008, https://doi.org/10.1088/1402-4896/ac0dfd.

[19] Asjad, M. I., Faridi, W. A., Jhangeer, A., Abu-Zinadah, H., & Ahmad, H. (2021). The fractional comparative study of the non-linear directional couplers in non-linear optics. *Results in Physics, 27*, 104459, https://doi.org/10.1016/j.rinp.2021.104459.

[20] Yao, S. W., Faridi, W. A., Asjad, M. I., Jhangeer, A., & Inc, M. (2021). A mathematical modelling of a Atherosclerosis intimation with Atangana-Baleanu fractional derivative in terms of memory function. *Results in Physics, 27*, 104425, https://doi.org/10.1016/j.rinp.2021.104425.

[21] Alam, M., Ilhan, O. A., Uddin, M., & Rahim, M. (2022). Regarding on the Results for the Fractional Clannish R andom Walker's Parabolic Equation and the Nonlinear Fractional Cahn-Allen Equation. *Advances in Mathematical Physics, 2022* Article ID 5635514, 12 pages. https://doi.org/10.1155/2022/5635514.

[22] Alam, M. N., Bonyah, E., & Fayz-Al-Asad, M. (2022). Reliable analysis for the Drinfeld-Sokolov-Wilson equation in mathematical physics. *Palestine Journal of Mathematics, 11*(1), 397–407

[23] Alam, M. N., Talib, I., Bazighifan, O., Chalishajar, D. N., & Almarri, B. (2021). An analytical technique implemented in the fractional Clannish R andom Walker's Parabolic equation with nonlinear physical phenomena. *Mathematics, 9*(8), 801, https://doi.org/10.3390/math9080801.

[24] Alam, M. N., Seadawy, A. R., & Baleanu, D. (2020). Closed-form wave structures of the space-time fractional Hirota–Satsuma coupled KdV equation with nonlinear physical phenomena. *Open Physics, 18*(1), 555-565.

[25] Bardin, B. S., & Chekina, E. A. (2019). On the constructive algorithm for stability analysis of an equilibrium point of a periodic hamiltonian system with Two Degrees of Freedom in the Case of Combinational Resonance. *Regular and Chaotic Dynamics, 24*(2), 127-144.

[26] Augner, B. (2019). Well-posedness and stability of infinite-dimensional linear port-Hamiltonian systems with nonlinear boundary feedback. *SIAM Journal on Control and Optimization, 57*(3), 1818-1844.

[27] Deffo, G. R., Yamgoue, S. B., & Pelap, F. B. (2018). Modulational instability and peak solitary wave in a discrete nonlinear electrical transmission line described by the modified extended nonlinear Schrödinger equation. *The European Physical Journal B, 91*(10), 1-9.

[28] Guy, T. T., & Bogning, J. R. (2018). Construction of Breather soliton solutions of a modeled equation in a discrete nonlinear electrical line and the survey of modulationnal instability. *Journal of Physics Communications, 2*(11), 115007, https://doi.org/10.1088/2399-6528/AAEAA1.

[29] Motcheyo, A. T., Tchawoua, C., & Tchameu, J. T. (2013). Supratransmission induced by waves collisions in a discrete electrical lattice. *Physical Review E, 88*(4), 040901, https://doi.org/10.1103/PhysRevE.88.040901.

[30] Zhou, X., Shan, W., Niu, Z., Xiao, P., & Wang, Y. (2018). Lie symmetry analysis and some exact solutions for modified Zakharov–Kuznetsov equation. *Modern Physics Letters B, 32*(31), 1850383, https://doi.org10.1142/S0217984918503839.

[31] Islam, S., Alam, M., Al-Asad, M., & Tunç, C. (2021). An analytical Technique for Solving New Computational Solutions of the Modified Zakharov-Kuznetsov Equation Arising in Electrical Engineering. *Journal of Applied and Computational Mechanics, 7*(2), 715-726.

[32] Linares, F., & Ponce, G. (2018). On special regularity properties of solutions of the Zakharov-Kuznetsov equation. *Communications on Pure & Applied Analysis, 17*(4), 1561–1572.

[33] Das, A. (2018). Explicit Weierstrass traveling wave solutions and bifurcation analysis for dissipative Zakharov–Kuznetsov modified equal width equation. *Computational and Applied Mathematics, 37*(3), 3208-3225.